Supplementary Methods

BrdU incorporation *in vivo*

In vivo bromodeoxyuridine (BrdU) incorporation was performed to analyze cell proliferation in the heart. Mice were subjected to LI-TAC, and 5 days later BrdU (100 mg/kg) was intraperitoneally administrated 2 h before sacrifice. Heart sections were then stained with anti-BrdU monoclonal antibody (Sigma).

Coculture of neonatal cardiomyocytes and adult cardiac fibroblasts

Thy1$^+$ cells were sorted from nonmyocyte-enriched cells isolated from adult mice. Neonatal cardiomyocytes were cultured in serum-free DMEM for 24 h in 3.5-cm culture dishes, after which the culture medium was replaced with fresh serum-free DMEM containing Thy1-positive adult cardiac fibroblasts (2.0×10^5 cells/dish). The ratio of fibroblasts to cardiomyocytes in the coculture was 50%, and the cells were cultured for an additional 24 h.

Migration assay

Cell migration was analyzed using Boyden chambers containing fluorescence-blocking filters with 8-μm pores (HTS fluoroblock, Falcon). Cardiac fibroblasts were cultured in serum-free DMEM for 24 h, after which they were harvested and resuspended in serum-free DMEM to a density of 1×10^6/ml. The cells were then stained with calcein acetoxymethyl ester, and 3×10^5 cells were added to the upper well of each Boyden chamber. To the lower well was added 1 ml of serum-free DMEM containing vehicle, IGF-1 or PDGF-A. The cells were allowed to migrate for 24 h at 37°C and then visualized by fluorescence microscopy.

BrdU incorporation *in vitro*

To analyze cell proliferation, *in vitro* bromodeoxyuridine (BrdU) incorporation was measured using a BrdU labeling and detection kit III (Roche). Cardiac fibroblasts were cultured in serum-free DMEM for 24 h, and then stimulated with vehicle, IGF-1 or PDGF-A. After incubation for 18 h at 37°C, the media were supplemented with 10 μM BrdU and incubated for an additional 6 h. The cells were then stained with a peroxidase-labeled antibody against BrdU. The absorbance of the samples at 405 nm with a reference wavelength of 490 nm was measured using a microplate reader (Bio-Rad, Model 680). The 405 nm/490 nm absorbance ratios were normalized to the ratios obtained with untreated cardiac fibroblasts.

Supplementary Figure Legends

Supplementary Figure 1

Pressure overload-induced cardiac hypertrophy after transverse aortic constriction.

Low-intensity (LI) and high-intensity (HI) TAC were accomplished by ligating the aorta against 25-gauge and 27-gauge needles, respectively. **(A)** Representative intraoperative pressure recordings measured in the right carotid artery. The aortas were tied firmly against the needles at the point shown by the arrowhead, after which the needles were removed (arrow). LI-TAC and HI-TAC produced different levels of pressure overload. **(B)** Representative low-magnification views of hematoxylin/eosin-stained heart sections 2 weeks after the sham operation or TAC. Scale bar, 1 mm. **(C-D)** Heart weight/body weight (HW/BW) ratios **(C)** and relative cross-sectional areas of left ventricular (LV) cardiomyocytes **(D)** 2 weeks after the sham operation or TAC. **(E)** Echocardiographic analysis of hearts 2 weeks after the operation: PWT, LV diastolic posterior wall thickness; LVDd, LV diastolic diameter; FS, fractional shortening. **(F)** Real-time PCR analysis of two cardiac hypertrophic marker genes, *Nppa* and *Myh7*. Expression levels of each gene were normalized to those of 18s ribosomal RNA and then further normalized to the levels in mice subjected to sham operations. *Nppa* encodes atrial natriuretic peptide; *Myh7* encodes cardiac β myosin heavy chain. $^{*}P<0.01$ vs. sham, $^{\#}P<0.05$ vs. LI-TAC. $n = 5$.

Supplementary Figure 2

Cardiac fibrosis induced by TAC.

(A) Representative low-magnification views of elastic picro sirius red-stained sections

of the left ventricles 2 weeks after the operations. Scale bar, 100 μm. **(B)** Fibrotic areas determined by elastic picro sirius red staining of cross-sections of hearts at the level of the papillary muscle. n=5 mice in each group. **(C)** Real-time PCR analysis of *Col1a1* expression. Expression levels were normalized to those of 18s ribosomal RNA and then further normalized to the levels in mice subjected to sham operations. $^{*}P<0.01$ vs. sham, $^{\#}P<0.01$ vs. LI-TAC. $n = 5$.

Supplementary Figure 3

Cardiac expression of *Klf5*.

(A-B) Expression of *Klf5* mRNA (**A**) and KLF5 protein (**B**) in hearts 3 days after the sham operation or LI-TAC. Expression levels were normalized to those of 18s ribosomal RNA and then further normalized to the levels in the mice subjected to sham operations **(A)**. $n = 3$. CBB, Coomassie Brilliant Blue staining of the gel. **(C)** Relative expression levels of *Klf5* in cultured neonatal cardiomyocytes and cardiac fibroblasts prepared from neonatal mice. Expression levels of *Klf5* mRNA were analyzed by real-time PCR and normalized to those of 18s rRNA and then further normalized to the levels in cardiomyocytes.

Supplementary Figure 4

Pressure overload-induced cardiac hypertrophy and fibrosis are attenuated in *Klf5*$^{+/-}$ mice.

Klf5$^{+/-}$ and wild-type (WT) mice were subjected to LI-TAC or sham operation as shown in Figure 1. **(A)** Echocardiographic analysis 2 weeks after the operations: PWT, LV diastolic posterior wall thickness; LVDd, LV diastolic diameter; FS, fractional shortening. **(B)** Real-time PCR analysis of marker genes for cardiac hypertrophy and

fibrosis in the hearts 14 days after the operations. Expression levels of each gene were normalized to those of 18s ribosomal RNA and then further normalized to the levels in mice subjected to sham operations. *Nppa* encodes atrial natriuretic peptide; *Myh7*, cardiac β myosin heavy chain; *Ctgf*, connective tissue growth factor; *Spp1*, secreted phosphoprotein 1; *Fn1*, fibronectin 1. $^{*}P<0.01$ vs. the sham control for the same genotype. $^{\#}P<0.05$ vs. WT subjected to TAC. $n = 7$.

Supplementary Figure 5

Generation of a *Klf5* conditional mouse line.

(A) Schematic representation of the targeting vector and expected gene replacement at the *Klf5* locus: H, *Hind*III; black triangles, loxP sequences; white triangles, FRT sequences. **(B)** Southern blot analysis of wild-type (WT), heterozygous floxed (Fl/+) and homozygous floxed (Fl/Fl) mice. Genomic DNA was digested with *Hind*III and subjected to hybridization with the probe indicated in **A**. The WT and floxed alleles produced 3.8 kb and 2.9 kb bands, respectively.

Supplementary Figure 6

Cardiomyocyte-specific *Klf5* deletion.

(A) Schematic representation of the floxed and floxed-out alleles and the primers used for genotyping. **(B)** Competitive PCR analysis of the floxed *Klf5* loci in cardiomyocytes isolated from adult $Klf5^{fl/fl}$ and $Klf5^{fl/fl}$;*αMHC-Cre* mice using the Langendorf isolation method. The primer set of A and B produced a 331-bp band for the floxed *Klf5* allele, while the primer set of B and C produced a 250-bp band for the floxed-out *Klf5* allele. **(C)** Real-time PCR analysis of *Klf5* expression in

cardiomyocytes isolated from *Klf5*$^{fl/fl}$ and *Klf5*$^{fl/fl}$;*αMHC-Cre* mice. $^{*}P<0.01$ vs. *Klf5*$^{fl/fl}$ mice. $n = 4$.

Supplementary Figure 7

Cardiomyocyte-specific deletion of *Klf5* does not alter pressure overload-induced cardiac hypertrophy and fibrosis.

Klf5$^{fl/fl}$ and *Klf5*$^{fl/fl}$;*αMHC-Cre* mice were subjected to LI-TAC or sham operation, as shown in Figure 2. **(A)** Echocardiographic analysis 2 weeks after the operations: PWT, LV diastolic posterior wall thickness; LVDd, LV diastolic diameter; FS, fractional shortening. **(B)** Real-time PCR analysis of cardiac hypertrophic and fibrotic marker genes. Expression levels of each gene were normalized to 18s ribosomal RNA levels. $^{*}P<0.01$ vs. the sham control for the same genotype. $n = 7$.

Supplementary Figure 8

Fibroblast-specific recombination by *Postn-Cre* transgenic mice.

(A) *LacZ* expression was visualized using X-gal in the heart from *R26RstoplacZ*;*Postn-Cre* mice subjected to sham operations as shown in Figure 3A. **(B-C)** Double-staining for β-galactosidase and isolectin B4 (brown) **(B)** or elastic picro sirius red staining **(C)** of LI-TAC hearts. Note that *lacZ* reporter gene expression was confined to fibroblasts. *LacZ* expression was detected throughout the fibrotic tissues, but was not observed in endothelial cells. Scale bars, 20 μm.

Supplementary Figure 9

Fibroblast-specific expression of β-galactosidase in *Klf5*$^{fl/fl}$;*Postn-Cre* hearts.

(A) Expression of β-galactosidase in cell populations enriched in either cardiomyocytes

or nonmyocytes isolated from *R26RstoplacZ*;*Postn-Cre* mice subjected to LI-TAC for 2 weeks. β-galactosidase activity was detected using the fluorescent substrate FDG. Note that addition of FDG did not alter the fluorescence in the myocyte population, while β-galactosidase$^+$ cells were clearly detected in the nonmyocyte population. (B) Expression of cell-lineage markers in β-galactosidase$^+$ cells sorted from the nonmyocyte population. Levels of mRNA expression of *Ddr2*, *Myh6* and *Cdh5* in β-galactosidase$^+$ cells (LacZ$^+$) normalized to those in adult Thy1$^+$ cardiac fibroblasts, cardiomyocytes (CM) and CD31$^+$ ECs. The expression levels in the control cells are the same as shown in Figure 3C.

Supplementary Figure 10

Fibroblast-specific *Cre* expression in *Postn-Cre* mice.

Relative levels of mRNA expression of *Cre* **(A)** and endogenous *Postn* **(B)** were assessed by real-time PCR in adult cardiomyocytes (CM), Thy1$^+$ fibroblasts and CD31$^+$ ECs isolated from *Klf5*$^{fl/fl}$ and *Klf5*$^{fl/fl}$;*Postn-Cre* mice 2 weeks after either the sham or LI-TAC operation. Cells were isolated as shown in Figure 3. $^*P<0.01$ vs. sham control for the same genotype in the same cell lineage group. $^\#P<0.01$ vs. *Klf5*$^{fl/fl}$ mice subjected to LI-TAC in the same cell lineage group.

Supplementary Figure 11

Suppression of fibrosis and fibroblast proliferation in *Klf5*$^{fl/fl}$;*Postn-Cre* mice.

Klf5$^{fl/fl}$ and *Klf5*$^{fl/fl}$;*Postn-Cre* mice were subjected to LI-TAC or sham operation, as shown in Figure 4. **(A)** Quantitative analysis of the expression of cardiac fibrosis-related marker genes: *Ctgf*, connective tissue growth factor; *Spp1*, secreted phosphoprotein 1; *Fn1*, fibronectin 1. The expression levels of each gene were

normalized to 18s ribosomal RNA levels and then further normalized to the levels in *Klf5*$^{fl/fl}$ mice subjected to the sham operation. n=7 mice for each group. **(B)** *In vivo* BrdU incorporation in hearts from *Klf5*$^{fl/fl}$ and *Klf5*$^{fl/fl}$;*Postn-Cre* mice subjected to LI-TAC or sham operation. BrdU was administered 2 h prior to sacrifice 5 days after the operations. Scale bar, 100 μm. $^{*}P<0.01$ vs. the sham control for the same genotype. $^{\#}P<0.05$ vs. *Klf5*$^{fl/fl}$ TAC. *n* =5 mice for each group.

Supplementary Figure 12

KLF5 is important for cardiomyocyte hypertrophy induced by coculture with adult cardiac fibroblasts.

Cultured neonatal cardiomyocytes were cocultured with Thy1^{+} cardiac fibroblasts isolated as shown in Figure 3B from *Klf5*$^{fl/fl}$ and *Klf5*$^{fl/fl}$;*Postn-Cre* mice subjected to LI-TAC for 2 weeks. Cardiomyocytes cultured without fibroblasts served as a control (CM). **(A)** Representative cardiomyocytes are shown stained for sarcomeric α-actinin (green). Nuclei were counterstained with Hoechst 33258 (blue). Scale bar, 10 μm. **(B)** Cell surface areas of 100 cells from each group. $^{*}P<0.05$ vs. cardiomyocytes alone. $^{\#}P<0.05$ vs. cells isolated from *Klf5*$^{fl/fl}$ mice subjected to LI-TAC.

Supplementary Figure 13

KLF5 knockdown does not alter *Postn* and *Tgfb3* expression in cultured cardiac fibroblasts.

KLF5 was knocked down using a specific siRNA as described in Figure 5A. Expression levels were normalized to those in cells transfected with the control siRNA (siCntrl).

Supplementary Figure 14

Differential effects of IGF-1 and PDGF-A on cardiomyocyte hypertrophy, and fibroblast proliferation and migration.

(A) Cultured cardiomyocytes were treated with the indicated concentrations of IGF-1 and PDGF-A for 24 h. Cell surface areas of 100 cardiomyocytes from each group are shown. **(B)** BrdU incorporation in cardiac fibroblasts treated with the indicated concentrations of IGF-1 and PDGF-A. $^{*}P<0.05$ vs. control. **(C)** Boyden chamber assays of the effects of IGF-1 and PDGF-A on migration of cardiac fibroblasts. The numbers of cells that migrated through porous membranes are shown. $^{*}P<0.01$ vs. cells migrated in SFM. n=4 wells each. Data are representative of 4 independent experiments.

Supplementary Figure 15

***Myh6* mRNA expression in nonmyocyte-enriched cell populations isolated from adult hearts.**

Levels of *Myh6* mRNA expression in nonmyocyte-enriched cell samples and in normal whole hearts. Expression levels were normalized to those of 18s rRNA, and then further normalized to that in whole hearts. $^{*}P<0.01$ vs. whole hearts.

Supplementary Figure 16

Levels of mRNA expression of KLF family members in *Klf5*-knockdown cardiac fibroblasts.

Mouse cardiac fibroblasts were transfected with either the siRNA for *Klf5* (siKlf5) or control siRNA (siCntrl) as described in Figure 5A. Expression levels of *Klf2*, *Klf4*,

Klf10, *Klf13* and *Klf15* were analyzed by real-time PCR, and were normalized to those in cells transfected with the control siRNA.

Supplementary Figure 17

***Igf1* mRNA variant containing exon 2 is preferentially expressed in cardiac fibroblasts.**

Numbers of *Igf1* transcripts containing exons 1 (class 1) or 2 (class 2) in cultured mouse cardiomyocytes and cardiac fibroblasts **(A)**, or in hearts before and 4 days after LI-TAC **(B)**, were analyzed using real-time PCR with external controls. The number of class 2 transcripts was normalized to that of class 1. As shown, class 2 transcripts are the major *Igf1* mRNA in the heart. $^{*}P<0.01$ vs. class 1. n = 3.

Supplementary Table 1

Real-time PCR analysis of secreted protein genes.

Genome-wide gene expression profiles in hearts 5 days after LI-TAC were analyzed using Affymetrix GeneChips. Genes encoding secreted proteins exhibiting significantly different expression levels in sham and LI-TAC hearts were selected. Genes encoding secreted proteins that did not show significantly different expression levels after the operations, but were previously suggested to be involved in cardiac hypertrophy were also analyzed. Changes in gene expression were analyzed by real-time PCR. Compared was gene expression in sham-operated and LI-TAC hearts, and in *Klf5*$^{fl/fl}$ and *Klf5*$^{fl/fl}$;*Postn-Cre* hearts subjected to LI-TAC. n=3, each group. **P*<0.05 vs. sham. $^{\#}$*P*<0.05 vs. *Klf5*$^{fl/fl}$. Expression levels in cultured cardiomyocytes and cardiac fibroblasts were also analyzed. n=5. $^{\$}$significantly enriched in fibroblasts, as compared to cardiomyocytes (*P*<0.05). Genes whose expression was significantly increased by LI-TAC, reduced in *Klf5*$^{fl/fl}$;*Postn-Cre*, or enriched in fibroblasts are shown in bold.

GenBank	Gene name	Gene symbol	Fold difference		
			TAC / Sham	*Klf5$^{fl/fl}$;Postn-Cre* / *Klf5$^{fl/fl}$*	fibroblast / myocyte
NM 009263	secreted phosphoprotein 1	Spp1	46.462*	0.824	0.943
NM015784	**periostin**	Postn	38.844*	0.432$^{\#}$	4.725$^{\$}$
NM 031168	interleukin 6	Il6	18.621*	1.202	0.930
NM 008726	natriuretic peptide precursor type B	Nppb	12.344*	0.844	0.011
NM 011333	chemokine (C-C motif) ligand 2	Ccl2	9.519*	0.699	0.368
NM 010809	matrix metallopeptidase 3	Mmp3	8.586*	0.605	0.323
NM 008501	leukemia inhibitory factor	Lif	6.384*	0.744	1.208
BC 004724	**fibronectin 1**	Fn1	6.260*	0.568$^{\#}$	9.125$^{\$}$
BG 075165	**insulin-like growth factor 1**	Igf1	6.149*	0.530$^{\#}$	3.783$^{\$}$
NM 010217	connective tissue growth factor	Ctgf	5.798*	0.611	1.674$^{\$}$
NM 009930	collagen, type III, alpha 1	Col3a1	5.626*	0.949	2.151$^{\$}$
NM 007742	**collagen, type I, alpha 1**	Col1a1	5.261*	0.550$^{\#}$	3.872$^{\$}$
NM 010415	heparin-binding EGF-like growth factor	Hbegf	4.770*	0.568	0.340
NM 008725	natriuretic peptide precursor type A	Nppa	4.709*	0.397$^{\#}$	0.050
NM 013693	tumor necrosis factor	Tnf	4.336*	0.707	0.217
NM 009367	transforming growth factor, beta 2	Tgfb2	3.966*	0.501$^{\#}$	1.098
NM 007993	**fibrillin 1**	Fbn1	3.525*	0.529$^{\#}$	4.993$^{\$}$
NM 008361	interleukin 1 beta	Il1b	2.938*	0.862	0.049
NM 013599	matrix metallopeptidase 9	Mmp9	2.669*	0.894	0.025
NM 133775	interleukin 33	Il33	2.009*	0.752$^{\#}$	0.063
NM 009368	**transforming growth factor, beta 3**	Tgfb3	1.872*	0.574$^{\#}$	2.074$^{\$}$
NM 010427	hepatocyte growth factor	Hgf	1.850*	0.746$^{\#}$	0.369
NM 011577	transforming growth factor, beta 1	Tgfb1	1.747*	0.802$^{\#}$	0.488
NM 010104	endothelin 1	Edn1	1.580*	1.044	1.451
NM 010798	macrophage migration inhibitory factor	Mif	1.222	0.745	0.441
NM 008808	platelet derived growth factor, alpha	Pdgfa	1.132	0.890	1.223
BC 061468	vascular endothelial growth factor A	Vegfa	1.037	0.878	0.664
BC 023427	platelet derived growth factor, B polypeptide	Pdgfb	1.002	0.765$^{\#}$	2.421$^{\$}$
NM 008610	matrix metallopeptidase 2	Mmp2	0.967	1.008	0.001
NM 008006	fibroblast growth factor 2	Fgf2	0.900	1.011	2.971$^{\$}$
NM 010514	insulin-like growth factor 2	Igf2	0.823	0.877	0.091
NM 007795	cardiotrophin 1	Ctf1	0.777	0.954	1.400

Supplementary Table 2

PCR primers.

Gene symbol	Forward primer	Reverse primer	Product size (bp)
Spp1	CTCAGAAGCAGAATCTC	ATGGTCTCCATCGTCATCAT	149
Postn	AACCAAGGACCTGAAACACG	GTGTCAGGACACGGTCAATG	170
Il6	AGTTGCCTTCTTGGGACTGA	TCCACGATTTCCCAGAGAAC	159
Nppb	CTGAAGGTGCTGTCCCAGAT	CCTTGGTCCTTCAAGAGCTG	185
Ccl2	AGGTCCCTGTCATGCTTCTG	TCTGGACCCATTCCTTCTTG	249
Mmp3	GGGATGATGATGCTGGTATGG	GCTTCACATCTTTTGCAAGGC	75
Lif	CGCCTAACATGACAGACTTCCCAT	AGGCCCCTCATGACGTCTATAGTA	193
Fn1	ACAGAAATGACCATTGAAGG	TGTCTGGAGAAAGGTTGATT	538
Ctgf	CCTGGTCCAGACCACAGAGT	GACAGGCTTGGCGATTTTAG	216
Col3a1	CCCAGAACATTACATACCA	GATTAAAACAAGATGAACAC	371
Col1a1	GCCAAGAAGACATCCCTGAAG	TCATTGCATTGCACGTCATC	139
Hbegf	GAAAGCAGGATCGAGTGAGC	CTTGCGGCTACTTGAACACA	221
Nppa	CCTAAGCCCTTGTGGTGTGT	CAGAGTGGGAGAGGCAAGAC	153
Tnf	AGCCCCCAGTCTGTATCCTT	CTCCCTTTGCAGAACTCAGG	213
Tgfb2	AAGTTTACACTGCCCCTGCTG	GGTGCCATCAATACCTGCAAA	103
Fbn1	CCCTGCGAGATGTGTCCTGC	TGTGTCCAGCGGGGCATTTG	175
Il1b	GCCCATCCTCTGTGACTCAT	AGGCCACAGGTATTTTGTCG	231
Mmp9	TGAATCAGCTGGCTTTTGTG	GTGGATAGCTCGGTGGTGTT	242
Il33	GGCTGCTTGCTTTCCTTATG	CCGTTACGGATATGGTGGTC	122
Tgfb3	GGAAGGCTGCACTCAGGAGA	CGGCCAGTTCATTGTGCTC	101
Hgf	TTCCCAGCTGGTCTATGGTC	TGGTGCTGACTGCATTTCTC	237
Tgfb1	AGGGCTACCATGCCAACTTCT	CCGGGTTGTGTTGGTTGTACA	102
Edn1	TTCCCGTGATCTTCTCTCTGCT	TCTGCTTGGCAGAAATTCCA	369
Mif	CCATGCCTATGTTCATCGTG	AGGCCACACAGCAGCTTACT	270
Pdgfa	CAGCATCCGGGACCTCCAGCGACTC	TCGTAAATGACCGTCCTGGTCTTGC	195
Vegfa	AACAAAGCCAGAAAATCACTGTGA	CGGATCTTGGACAAACAAATGC	67
Pdgfb	CCCACAGTGGCTTTTCATTT	GTGGAGGAGCAGACTGAAGG	206
Mmp2	ATCGCTCAGATCCGTGGTG	TGTCACGTGGTGTCACTGTCC	73
Fgf2	GACCCCAAGCGGCTCTACTGC	GTGCCACATACCAACTGGAGT	307
Igf2	CAGCGGCCTCCTTACCCAACT	GAGGTAGACACGTCCCTCTCG	321

Ctf1	GAGGGATACGTGCAGCAACA	GGCCAGCACTGTCTCCAC	288
Myh6	CCAATGAGTACCGCGTGAA	ACAGTCATGCCGGGATGAT	236
Myh7	ATGTGCCGGACCTTGGAA	CCTCGGGTTAGCTGAGAGATCA	148
Klf2	ACCAAGAGCTCGCACCTAAA	GTGGCACTGAAAGGGTCTGT	156
Klf4	CTGAACAGCAGGGACTGTCA	GTGTGGGTGGCTGTTCTTTT	218
Klf5	TGGTTGCACAAAAGTTTATAC	GGCTTGGCGCCCGTGTGCTTCC	162
Klf10	AGCAAGGGTCACTCCTCAGA	ACATGGGACAGGCAAACTTC	239
Klf13	GGAAATCTTCGCACCTCAAG	GGCAGCTGAACTTCTTCTCG	153
Klf15	TCATGGAGGAGAGCCTCTGT	TCTCCCAGCAGACTCTGGAT	249
Ddr2	CCTATGTCCTTGGGCACTGT	CTGCCAGCCTACTCAAGTCC	196
Cdh5	ATTGAGACAGACCCCAAACG	TTCTGGTTTTCTGGCAGCTT	239
Cre	CGATGCAACGAGTGATGAGG	GCATTGCTGTCACTTGGTCGT	250

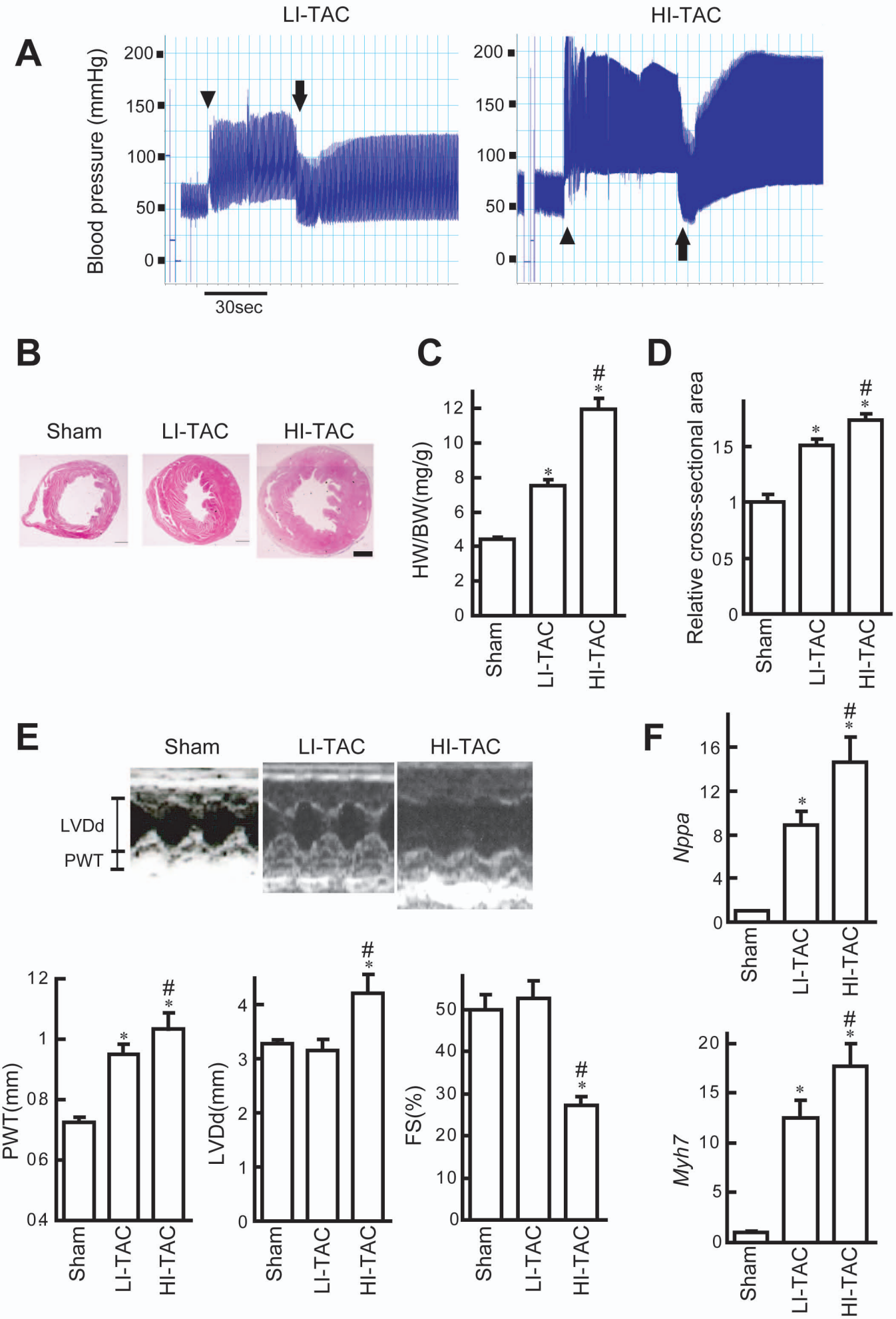

Supplementary Figure 1

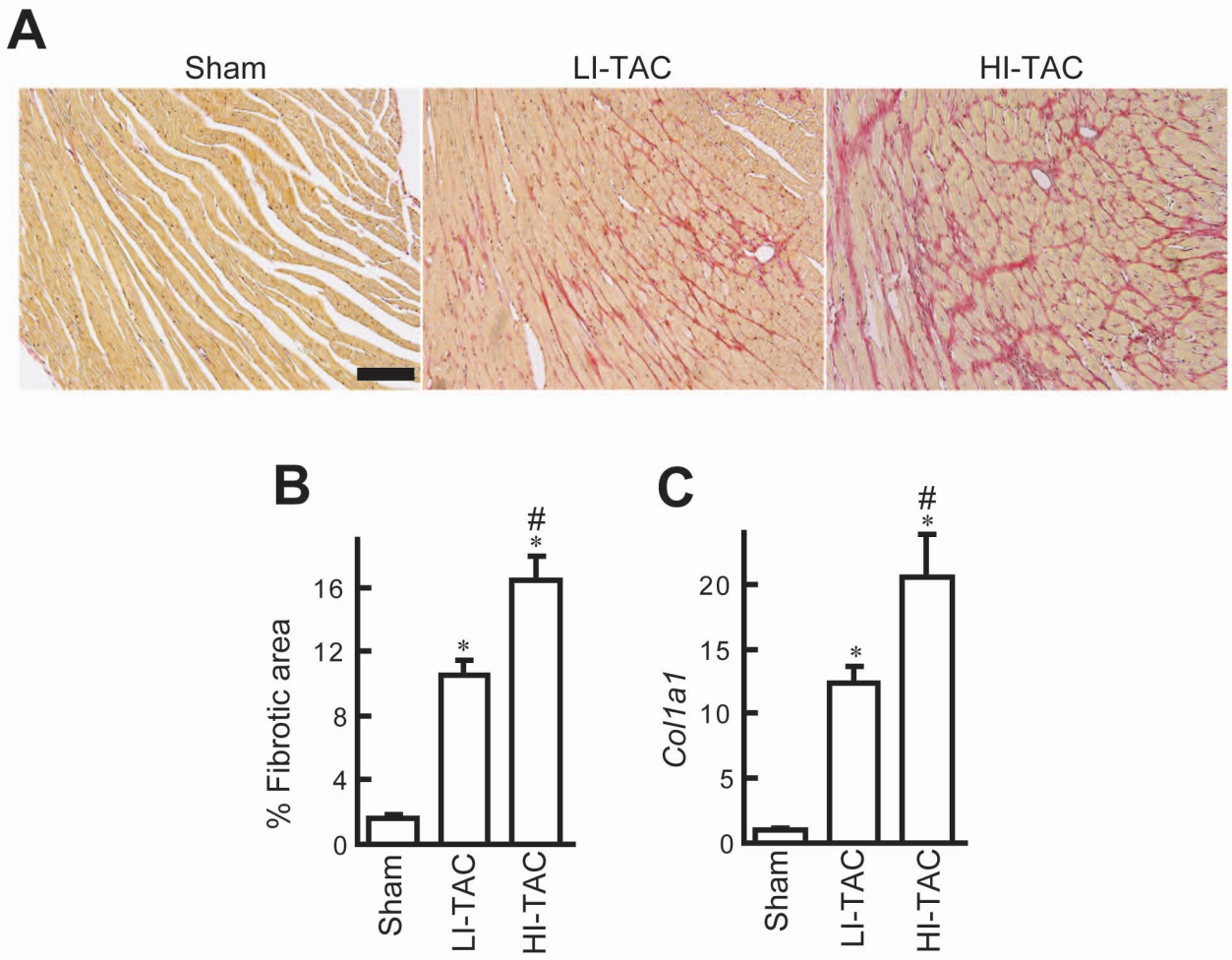

Supplementary Figure 2

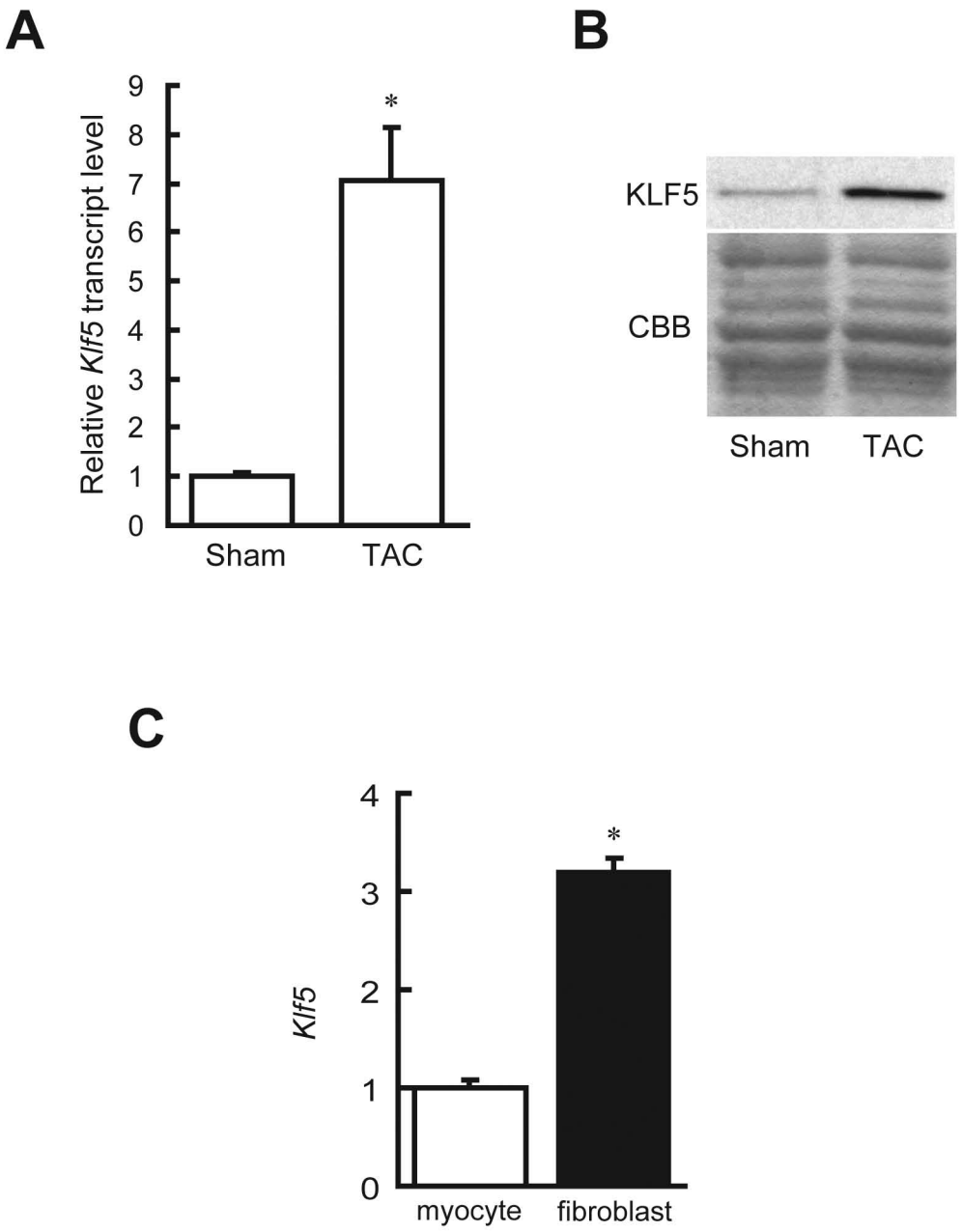

Supplementary Figure 3

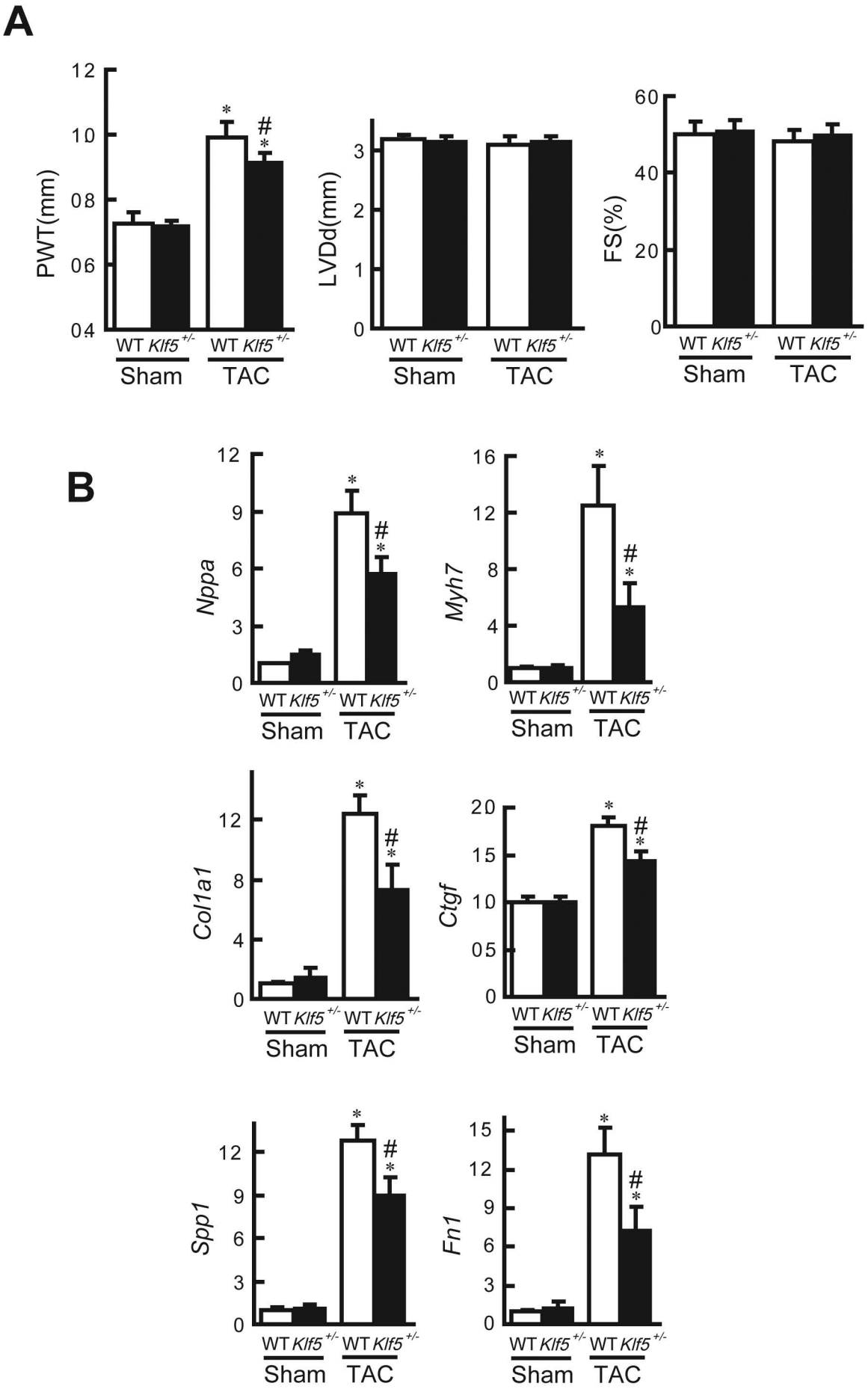

Supplementary Figure 4

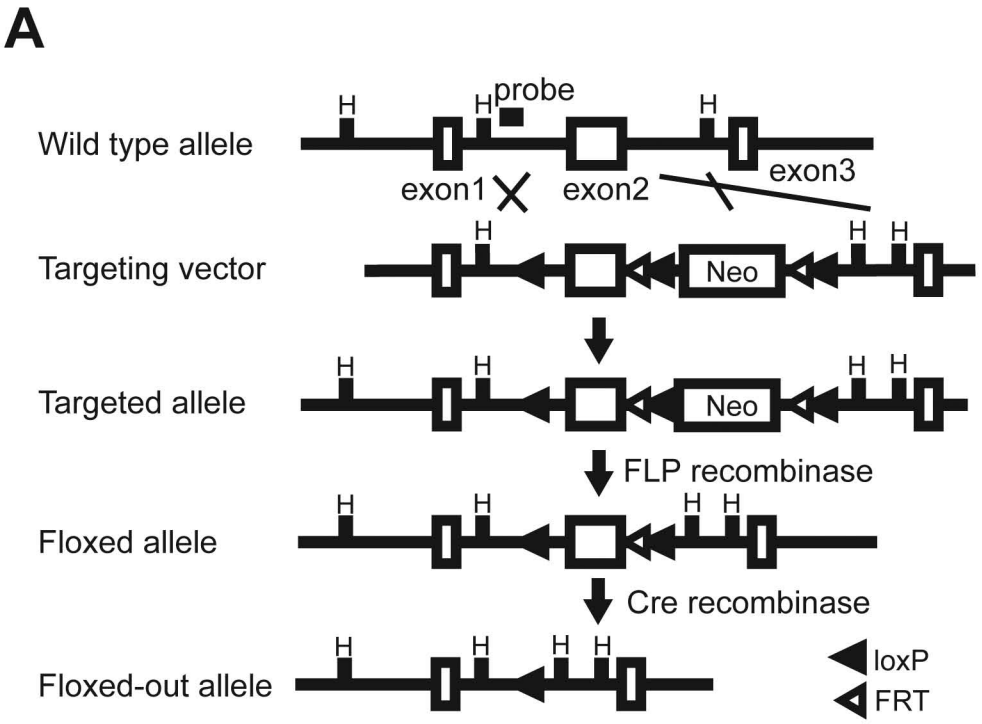

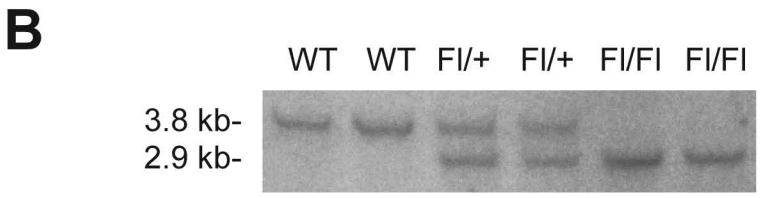

Supplementary Figure 5

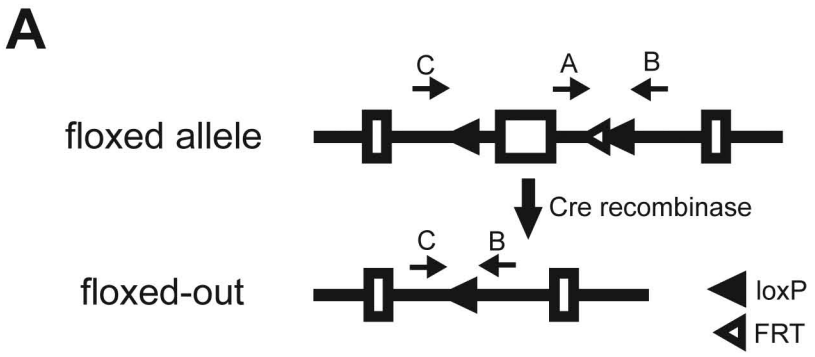

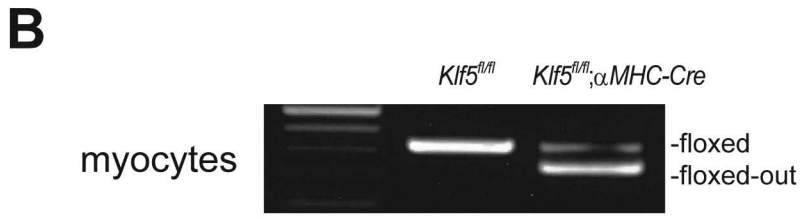

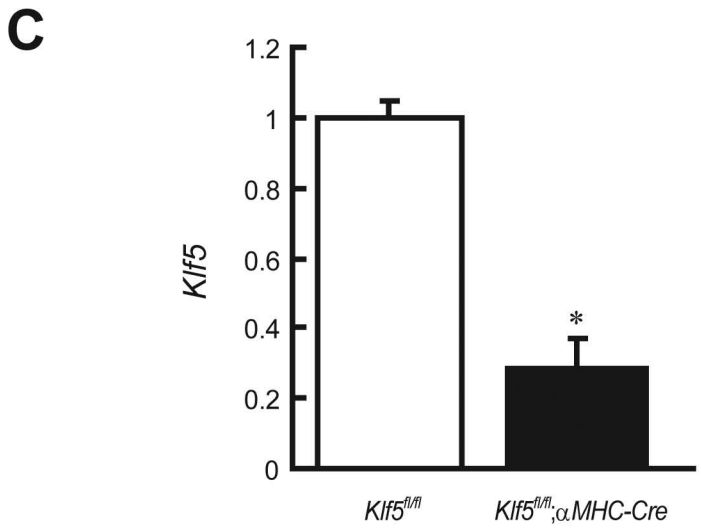

Supplementary Figure 6

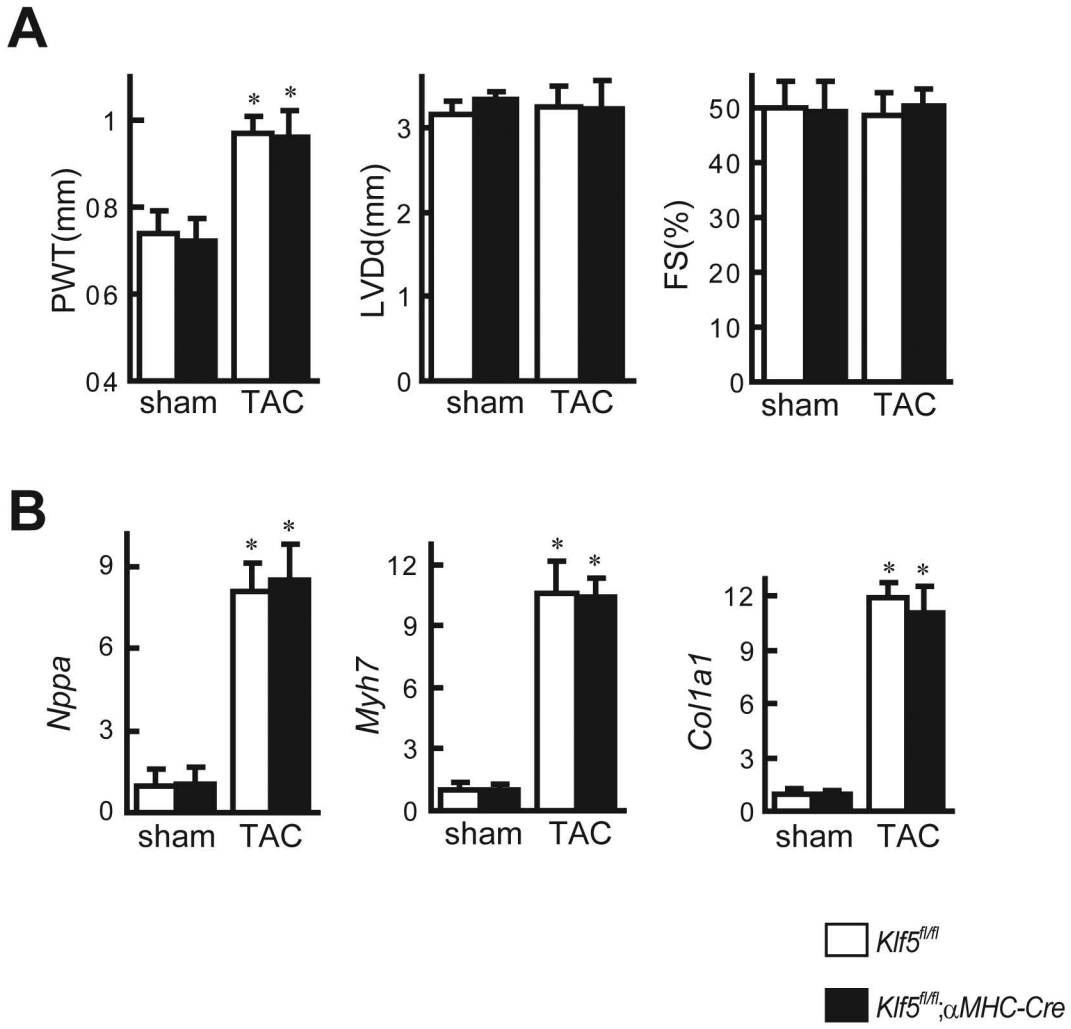

Supplementary Figure 7

A

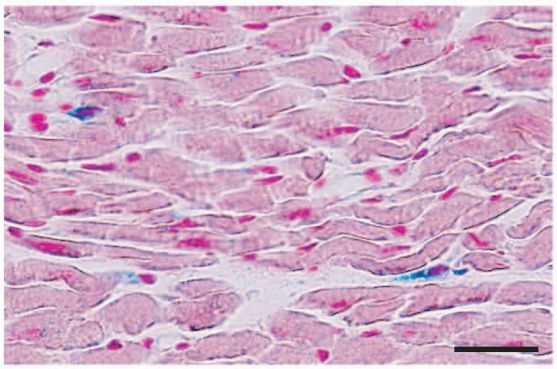

B

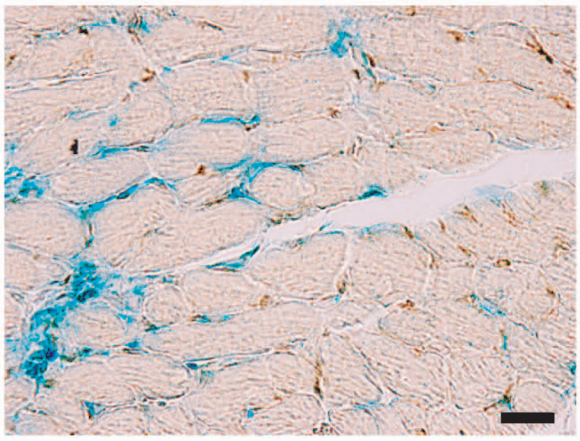

C

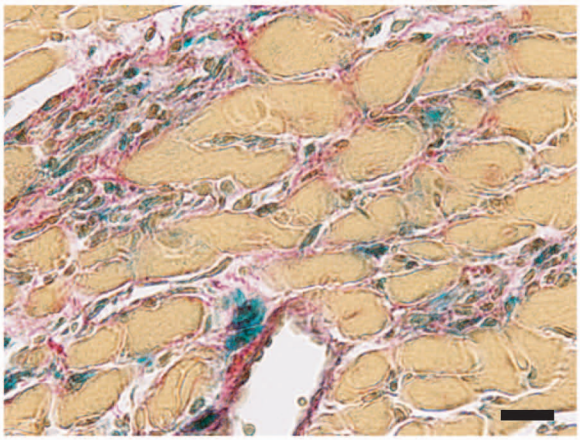

Supplementary Figure 8

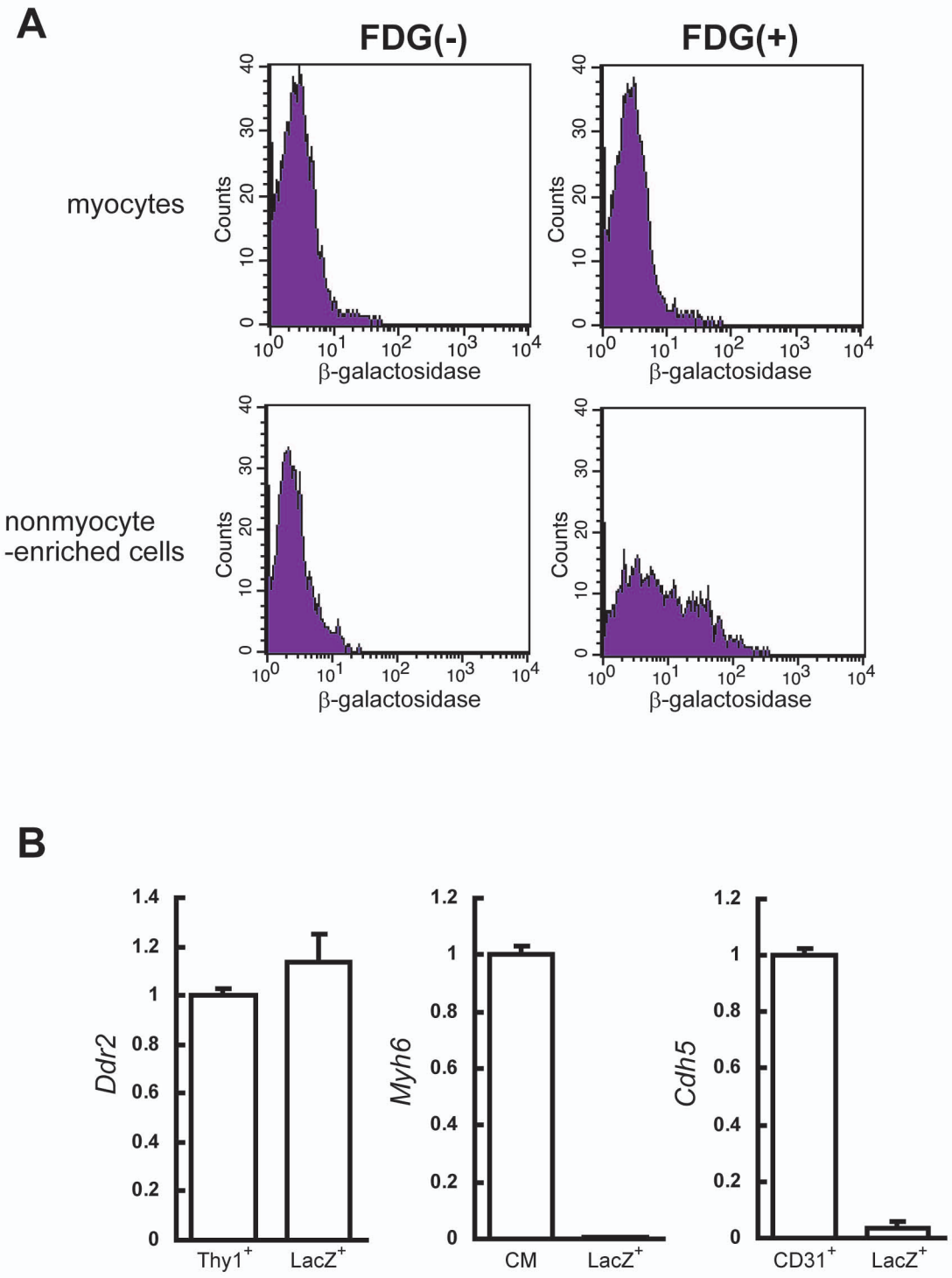

Supplementary Figure 9

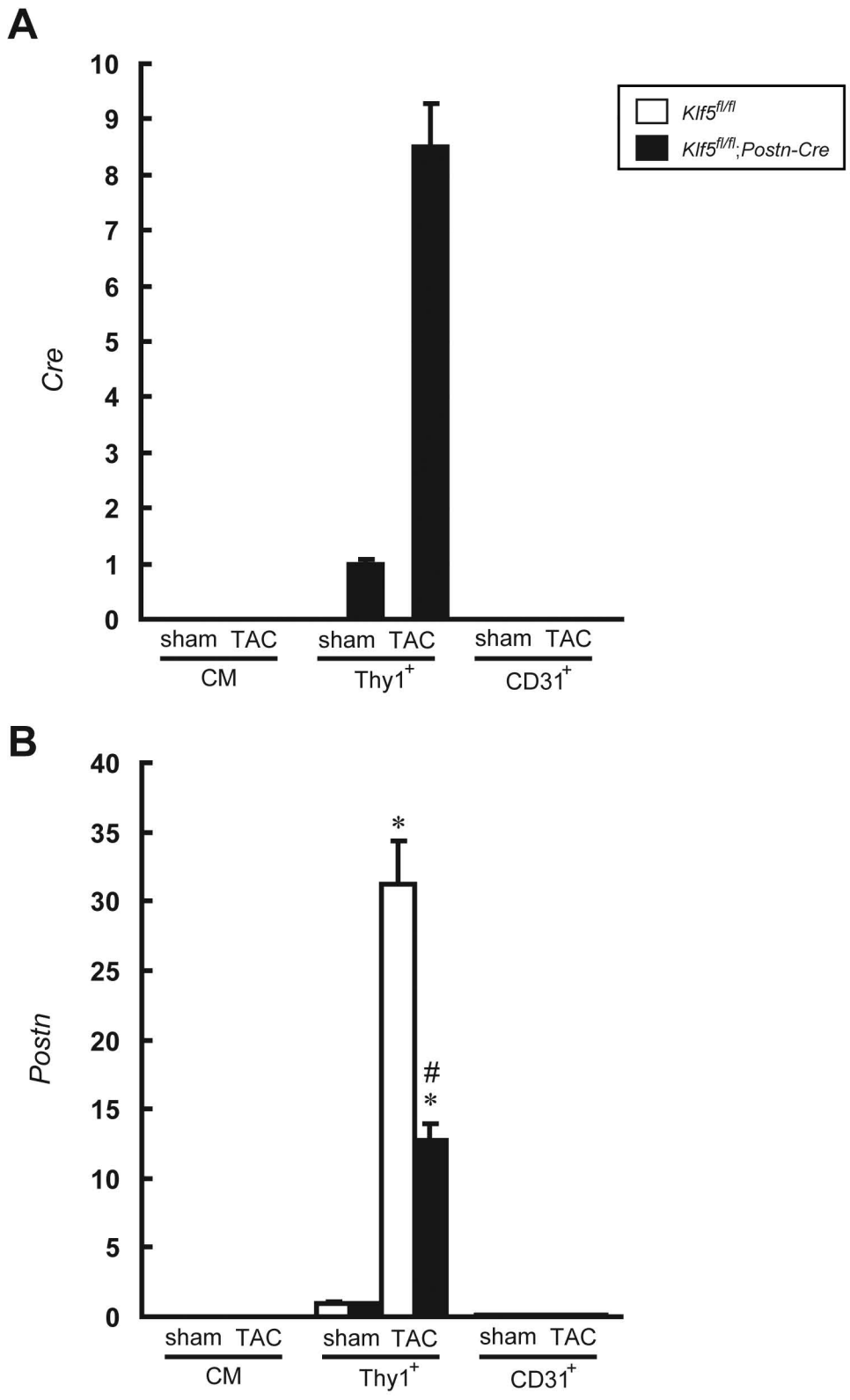

Supplementary Figure 10

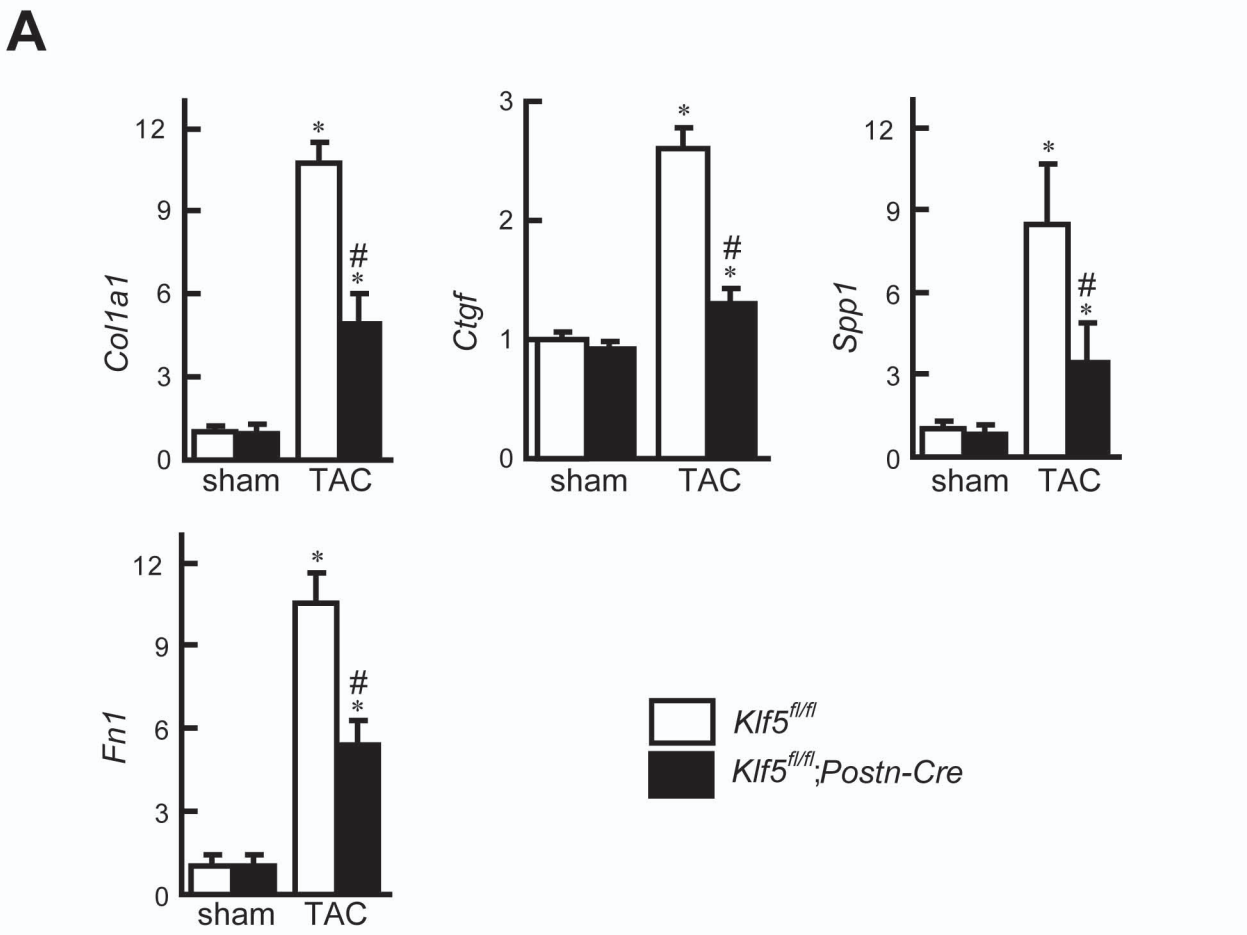

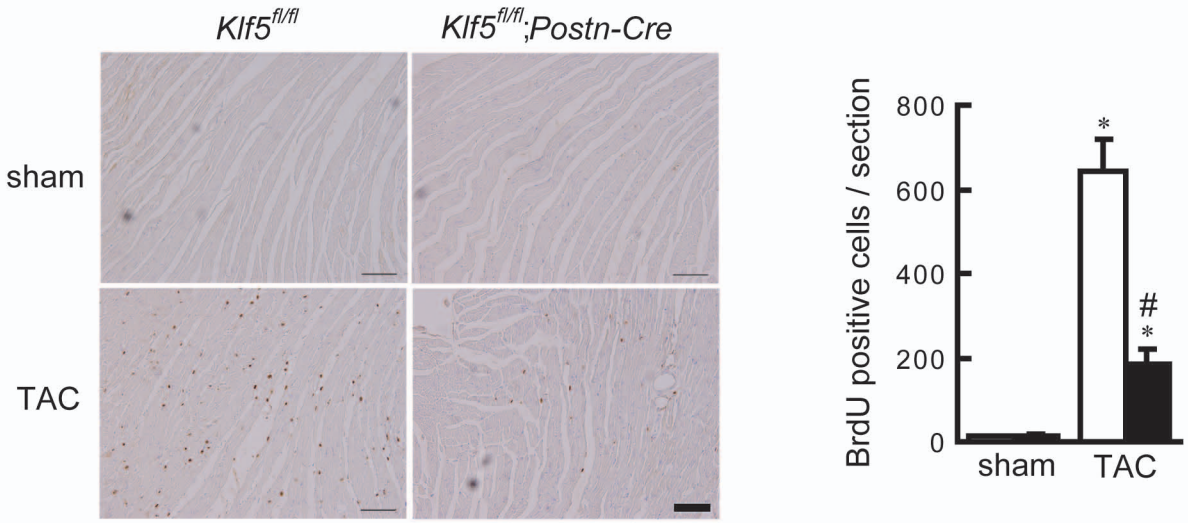

Supplementary Figure 11

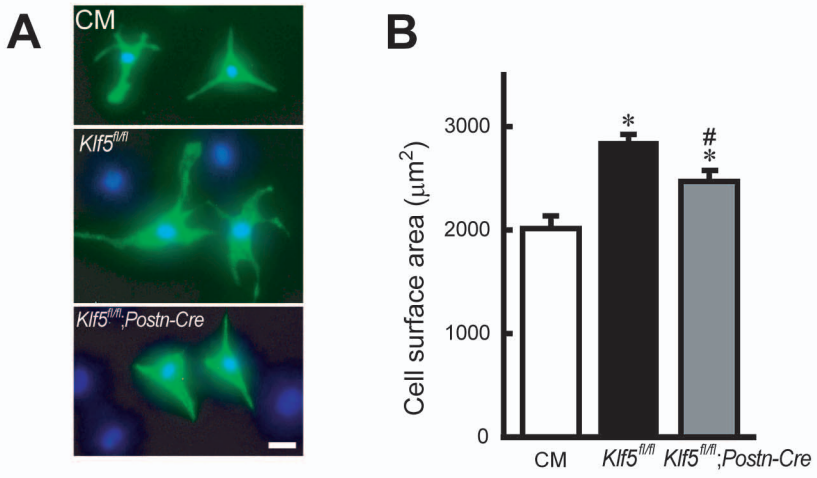

Supplementary Figure 12

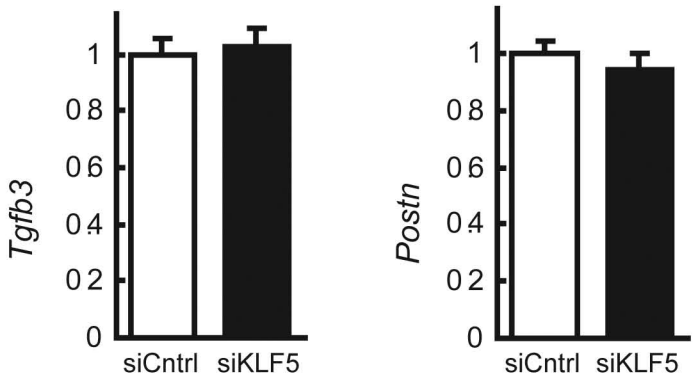

Supplementary Figure 13

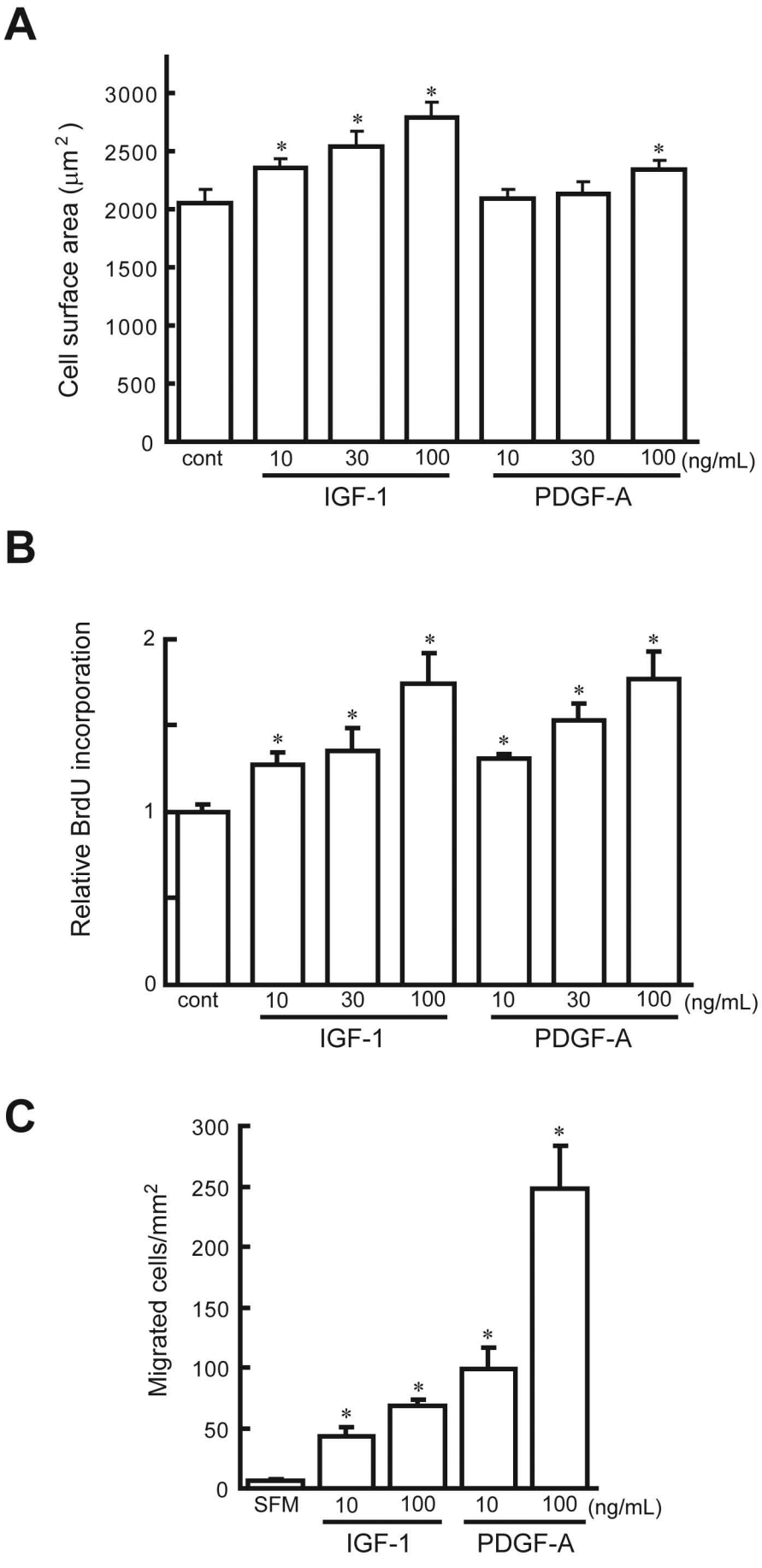

Supplementary Figure 14

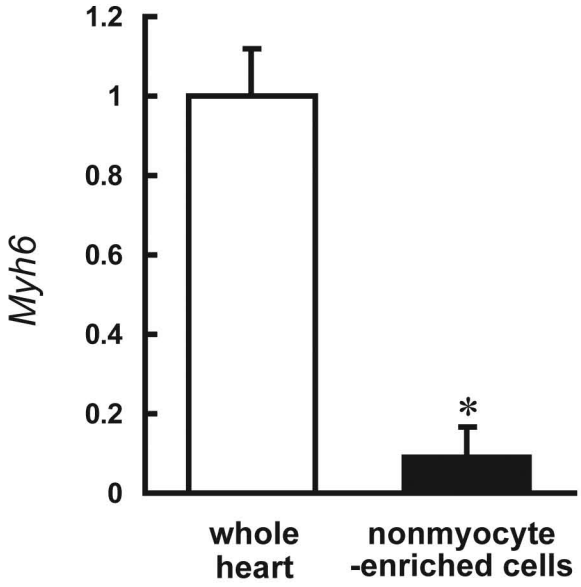

Supplementary Figure 15

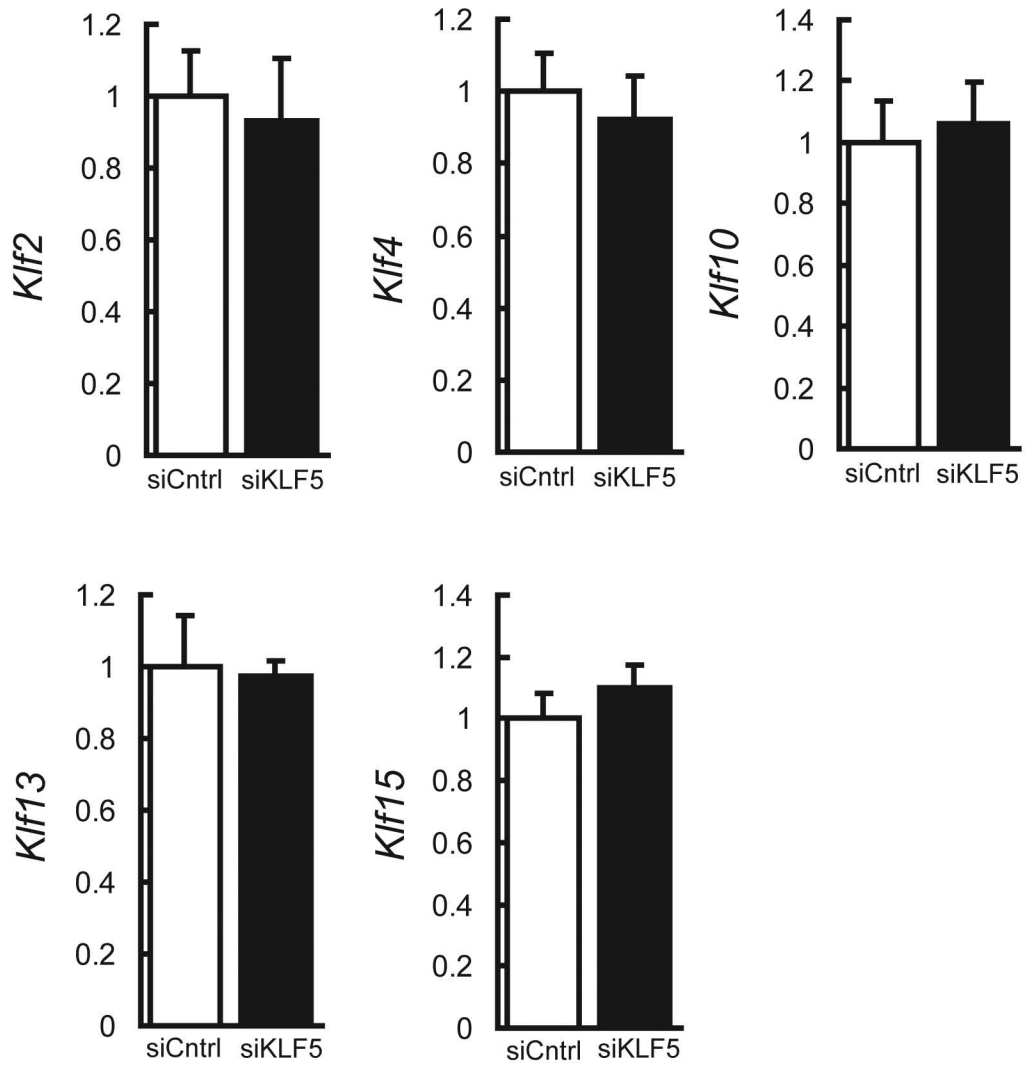

Suppelmentary Figure 16

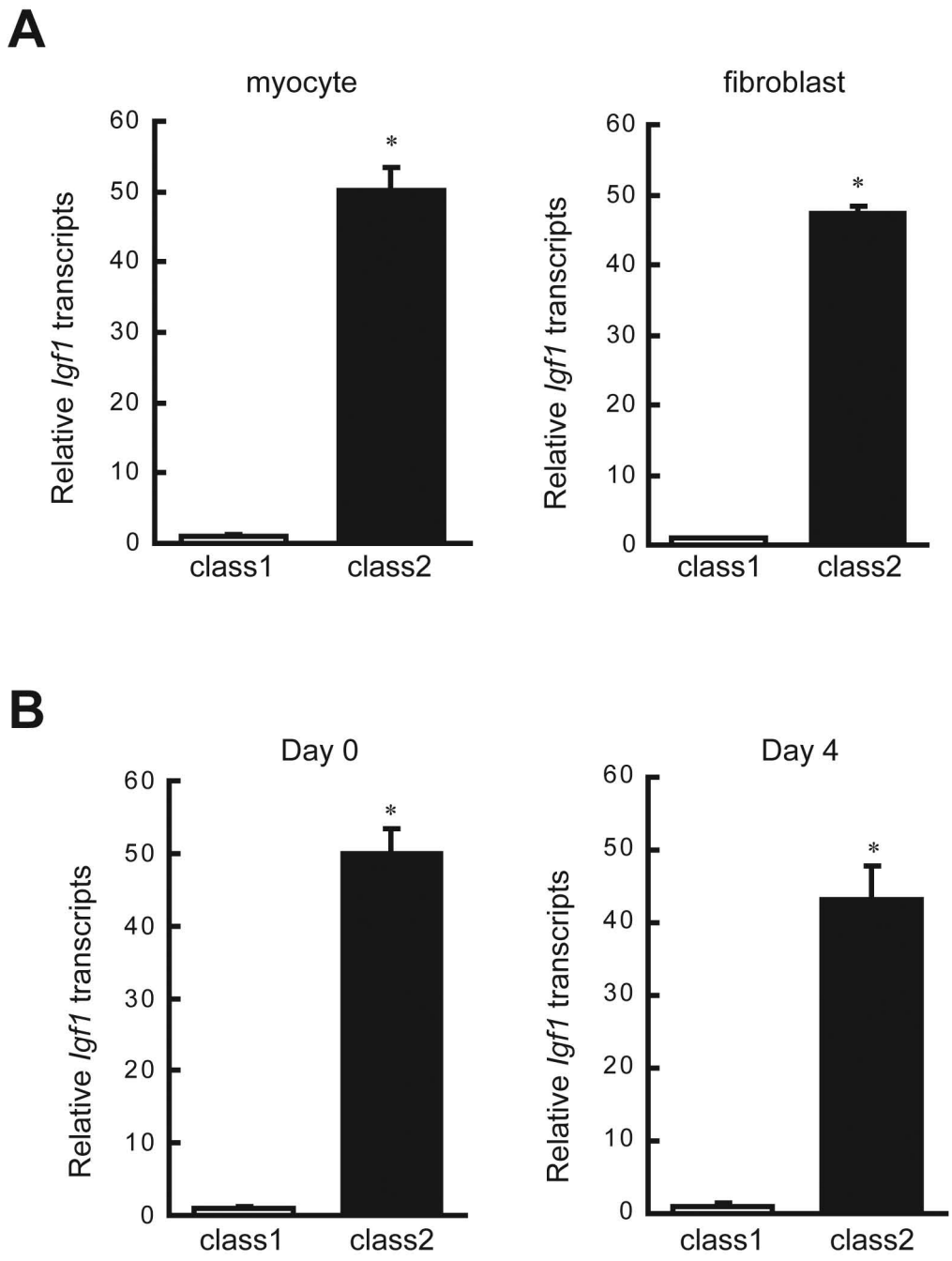

Supplementary Figure 17